

# ON STOCHASTIC DYNAMIC PREDICTION

## II. Predictability and Utility

REX J. FLEMING

Air Weather Service, U.S. Air Force<sup>1</sup>

### ABSTRACT

The stochastic dynamic equations, as investigated in part I of this two-part study, can be applied to any time-dependent set of differential equations which are, at most, nonlinear quadratic. In this study, they are used to explore various aspects of the question of atmospheric predictability.

The growth of uncertainty due to ill-defined initial conditions in the nonlinear advection field is viewed by considering a simple barotropic model. A wave number is defined to be "unpredictable" when the "uncertain" energy associated with that wave becomes as large as the "certain" energy associated with it. The predictability of wave number 12 is used as a reference point and as an arbitrary minimum requirement for useful synoptic forecasts. It is found that, based upon the average root-mean-square vector error in the wind field today, such a wave number has a predictability value of about 1.5 days. If this error could be reduced by a factor of 4 (i.e., down to 1 m/s), this value would be approximately 5 days. Using a stochastic barotropic model with 2,015 degrees of freedom, it is found that any initial energy spectra for the certain or uncertain eddy kinetic energy will give essentially the same predictability values. This is because the complete nonlinearity is accounted for in the stochastic dynamic equation set and the dynamics of the two-dimensional fluid tend to drive any initial spectrum into approximately a  $-3$  power law in some averaged sense—as expected from theory.

It is shown that the rather pessimistic predictability values, based solely upon error growth due to uncertain advection and instability processes, are considerably lengthened (at least in the largest scales) when additional forcing and dissipation terms are included in the mathematical models. However, such additional forces can never be simulated perfectly and the qualitative effect of these imperfections is shown by calculations with a simple baroclinic model having heating and friction. Based upon arguments presented, the author speculates that in 10 yr the projected uncertainties in the physics and the uncertainties arising from the computational wave number cutoff will still restrict the predictability of wave number 12 to within 5–7 days. It is shown how the eventual application of the stochastic dynamic equations to more complicated models can replace such speculation with more concrete evidence.

The globally averaged value of predictability considered above is very general and it is shown how the utility of the stochastic dynamic set can provide more meaningful information to the user. Only one aspect of this utility is shown (the growth of the phase error of a wave with time), but the stochastic set of equations gives the "believability" of each variable at every point in the space-time domain.

### 1. INTRODUCTION

This study attempts to add to the theory of atmospheric predictability. The complete question of predictability, with its different meanings to different users, applied to various scales of atmospheric features, is not likely to be completely answered in the near future. Yet, the importance of knowledge about predictability cannot be stressed too much. The present volume and quality of observations that are useful for predicting the atmosphere are far from adequate. The quality of that data available in the next decade from the Global Atmospheric Research Program (GARP) will still be far from adequate. It is the author's opinion that, although the science of meteorology has grown tremendously over the past century, the expanding "economic effort" in observing the atmosphere has not kept pace with the expanding "economic value" in knowing what the atmosphere is going to do.

The science of numerical weather prediction, that is, the application of computers to solve the mathematical equations describing the physics of the atmosphere, forms the basis of nearly all statements about the future condition of the atmosphere. But, because the initial features of the atmosphere are so ill-defined in the "medium" or synoptic

scales and not defined at all in the smaller scales, the numerical forecast rapidly deteriorates. Now if, by a proposed increase of the observations with the purpose of better defining atmospheric features down to some arbitrary scale, one could put a "dollar value" on the improvement of the forecast, then that would be justification for more observations. Improved observations alone, however, will not provide *definitive* statements about forecast improvements. Because the equations are nonlinear and because the scales of features smaller than that chosen arbitrary scale would still not be known, only *estimates* of the improvement of the forecasts can be made. The nonlinear interactions between scales (known and unknown), coupled with physical forces which are not "perfectly" simulated, produce the uncertainty and make statements of predictability only "speculation" when the usual meteorological equations are used.

The stochastic approach to atmospheric prediction is capable of reducing that speculation of predictability. This approach was introduced by Epstein (1969) and is expanded upon in part I of this study (Fleming 1971).

It was shown in part I that the general deterministic prognostic equation given by Lorenz (1963a)

$$\dot{X}_i = \sum_{p,q} a_{ipq} X_p X_q - \sum_p b_{ip} X_p + c_i \quad (1)$$

<sup>1</sup> Now assigned to the National Meteorological Center, National Weather Service, NOAA, Suitland, Md.

can be considered a subset of the general stochastic set of equations

$$\dot{\mu}_i = \sum_{p,q} a_{ipq}(\mu_p \mu_q + \sigma_{pq}) - \sum_p b_{ip} \mu_p + c_i, \quad (2)$$

$$\dot{\sigma}_{ij} = \sum_{p,q} [a_{ipq}(\mu_p \sigma_{jq} + \mu_q \sigma_{jp} + \tau_{j pq}) + a_{jqp}(\mu_p \sigma_{iq} + \mu_q \sigma_{ip} + \tau_{i pq})] - \sum_p (b_{ip} \sigma_{jp} + b_{jp} \sigma_{ip}), \quad (3)$$

and

$$\begin{aligned} \dot{\tau}_{jki} = & \sum_{p,q} [a_{jpq}(\mu_p \tau_{k l q} + \mu_q \tau_{k l p} + \sigma_{kp} \sigma_{l q} + \sigma_{kq} \sigma_{l p}) \\ & + a_{k p q}(\mu_p \tau_{j l q} + \mu_q \tau_{j l p} + \sigma_{jp} \sigma_{l q} + \sigma_{jq} \sigma_{l p}) \\ & + a_{l p q}(\mu_p \tau_{j k q} + \mu_q \tau_{j k p} + \sigma_{jp} \sigma_{k q} + \sigma_{jq} \sigma_{k p})] \\ & - \sum_p (b_{jp} \tau_{k l p} + b_{kp} \tau_{j l p} + b_{lp} \tau_{j k p}) - K \tau_{jki} \end{aligned} \quad (4)$$

where

- ( $\dot{\phantom{x}}$ ) refers to a time derivative,
- $p$  and  $q$  are dummy indices,
- $X_i$  is a dependent variable,
- $\mu_i$  is the mean of  $X_i$ ,
- $\sigma_{ij}$  is the variance if  $i=j$  and covariance if  $i \neq j$ ,
- $\tau_{ijk}$  is the instantaneous third moment about the mean, and
- $a, b, c,$  and  $K$  are constants.

The closure of this set was discussed in part I. We shall also include calculations in this study that use the closure scheme of Epstein (1969) which simply assumes that third moments about the mean in eq (3) are zero, thus eliminating the need for eq (4).

The spectral equations of a two-level model used to investigate stochastic concepts were fully described in part I and are only repeated here for reference. These are

$$\dot{\psi}_i = \sum_{p,q} a_{ipq}(\psi_p \psi_q + \theta_p \theta_q) - b_i(\psi_i - \theta_i) \quad (5)$$

and

$$\dot{\theta}_i = \sum_{p,q} (a'_{ipq} \theta_p \psi_q + a''_{ipq} \psi_p \theta_q) - b'_i \psi_i - b''_i \theta_i + c_i \theta_i^* \quad (6)$$

where  $\psi$  is a stream function representing the mean wind,  $\theta$  represents the mean potential temperature,  $\theta^*$  is a preassigned temperature field, and  $a, a', a'', b, b', b'',$  and  $c$  are constants.

These quite simple equations, which are a particular form of the general form [eq (1)], will be used to illustrate various aspects of predictability that can be directly handled by the stochastic dynamic method. It would obviously be more desirable to use a more complicated set of deterministic equations, more representative of the atmosphere, as a basis. However, the limited computer power available to meet the computational demands of the stochastic dynamic equation set restricts us to this simple model, at least in this study. We might point out that Monte Carlo calculations, similar to those described

in part I, could have been used to investigate predictability. Approximate results, using a small sample size, could be obtained at less computer cost. However, this computational advantage is reduced when the uncertainties of the external forcing parameters are included in predictability calculations. This additional source of uncertainty is conveniently handled by the stochastic dynamic approach. Further, the stochastic approach is mathematically more elegant than the Monte Carlo (treating the low order moments as predictable entities rather than as indirectly computable quantities) and gives more accurate information on how the variables are related (unless a large sample size is used in the Monte Carlo calculations).

## 2. BAROTROPIC PREDICTABILITY

There can be so many definitions of predictability, based upon what is being forecast and how the forecast is being used, that no attempt is made to review these. The primary definition used in this study which most closely resembles the definitions of others (concerned with predictability of the atmosphere as a whole—stated in general terms or partitioned according to scale) is that any atmospheric scale of motion, represented by a wave number, becomes “unpredictable” when the uncertain kinetic energy becomes greater than the certain kinetic energy; that is, when  $(UK_E/K_B) > 1$ . All types of energy; certain and uncertain, are defined and described in part I.

We should emphasize that this definition is related to the “precision” with which the mathematical model can specify the future position of an atmospheric feature in the space-time domain. However, there are a number of users of meteorological information who do not require “precise” forecasts and who would perhaps base predictability on utility over an extended period in the time domain, thus arriving at longer predictability times than given here. The stochastic equations would give perfect input into a particular utility matrix to arrive at such a determination of predictability, but this topic will not be pursued here.

The above definition is similar to that used by Lorenz (1969). He considered the barotropic vorticity equation

$$\frac{\partial(\nabla^2 \psi)}{\partial t} = -J(\psi, \nabla^2 \psi). \quad (7)$$

He then considered two separate fields of flow,  $\psi$  and  $\psi + \epsilon$ , for which the difference  $\epsilon$  is governed by the equation

$$\frac{\partial(\nabla^2 \epsilon)}{\partial t} = -J(\psi, \nabla^2 \epsilon) - J(\epsilon, \nabla^2 \psi) - J(\epsilon, \nabla^2 \epsilon). \quad (8)$$

Lorenz then assumed that the “error,”  $\epsilon$ , was small compared to  $\psi$  so that it was governed by the *linearized* equation

$$\frac{\partial(\nabla^2 \epsilon)}{\partial t} = -J(\psi, \nabla^2 \epsilon) - J(\epsilon, \nabla^2 \psi) \quad (9)$$

TABLE 1.—*Barotropic predictability given by stochastic dynamic equations and by Lorenz (1969)*

Wave number source	Wave number prediction	Stochastic dynamic (days)	Lorenz (-5/3) (days)
(2, 4, 6)		7.5	
(4, 8, 12)	4		4.0
(2, 4, 6)		4.3	
(6, 12, 18)	6	4.5	3.0
(4, 8, 12)	8	3.5	2.0
(4, 8, 12)	12	2.3	1.5
(6, 12, 18)		2.1	

until such time that  $\epsilon$  is not small. Lorenz considered a statistical ensemble of  $\psi$  and  $\epsilon$ , then using the linearized eq (9) he incorporated a number of assumptions to arrive at a single equation for the evolution of the error kinetic energy.

Lorenz discussed these assumptions and realized their limitations. Some of the limitations of the method are assumptions of homogeneity and isotropy, the neglect of a prognostic equation for covariances, the use of a pre-defined energy spectrum function, and the use of the linearized error equation itself. The stochastic dynamic approach need not resort to any of the above assumptions although the question of closure must be faced. The stochastic dynamic equations will be applied to the barotropic vorticity equation and a comparison with the results of Lorenz will be given in table 1.

The same barotropic vorticity equation used by Lorenz [eq (7)] can be obtained from eq (5) by setting the  $\theta_i$  and  $b_i$  equal to zero. There are, of course, many possible initial conditions that one could begin with. The calculations in this study indicate that, at least as far as predictability as defined here is concerned, the initial values of  $\psi$  do not make too much difference in the results. The purpose of numerical calculations in this study is to give a qualitative indication of predictability based on "representative" atmospheric values. In this section, our model still has only three longitudinal waves (usually all of low wave numbers). With this in mind, we simply choose initial values of  $\psi_i$  in such a way that, whatever set of waves is considered, each wave will have the same amount of certain energy to begin with. The energy distribution between wave numbers will then evolve according to the dynamics. This energy adjustment takes place rapidly (as indicated in a later section) and has little effect on predictability here. The initial uncertain energy in a wave number will be a small percentage (usually 1 percent) of the certain energy in the corresponding wave number.

The initial conditions are arbitrarily chosen to give typical values of the zonal flow and eddy amplitudes as might be found in the atmosphere at 500 mb. The initial energies per unit mass per unit area are:  $K_z=100$ ,  $K_E=100$ ,  $UK_z=1$ , and  $UK_E=1$ . All energy values are in the

units of  $m^2 \cdot s^{-2}$  per unit area. The zonal energy is split into 80 units in mode 1 and 20 units in mode 2. The variance of each component being 1/100 of its respective mean value results in a standard deviation of 10 percent for each component. Lorenz confined the error to a single wave (the smallest or largest with essentially similar results) while this calculation has errors in all waves considered. The details of Lorenz' initial conditions would require an explanation of some of the assumptions and can be referred to in his 1969 paper.

The model previously described in detail contained only three waves in the  $x$ -direction. Values of predictability for a given wave number are computed from two different sets where possible. Results for several waves are shown in table 1 with the predictability expressed in days. Direct comparison to the results of Lorenz (1969) can only be made for certain wave numbers (his  $k=1, 2, 3, 4, 5, \dots$ , correspond to our wave numbers 1, 2, 4, 8, 16, . . .), but interpolation of his results for those wave numbers is sufficiently accurate for a general comparison. Lorenz considered cases of the energy spectra obeying  $-5/3$  and  $-7/3$  power laws. However, to agree in initial root-mean-square velocity error, we must use the results from his application of the  $-5/3$  power law. His experiment "C3" is in close agreement with our initial error.

The results show that the stochastic dynamic predictability values are larger than those indicated by Lorenz. However, had Lorenz used a  $-3$  power law that is deduced by Leith (1968) and observed in atmospheric data as shown by Wiin-Nielsen (1967) and by Julian et al. (1970), his predictability ranges would be considerably longer. The stochastic approach allows for a nonlinear error growth. Thus, with uncertainty in the zonal flow, the barotropic instability mechanism accelerates error growth in some waves as discussed in part I. Such a mechanism is absent from Lorenz' approach because of his assumptions of homogeneity and isotropy. On the other hand, it was shown in part I that there is an energy flow between certain and uncertain components that takes place in the stochastic dynamic model so that there is a feedback of uncertain energy into certain energy. This is from the stable waves which tend to slow down the error growth.

The above calculations used the simple closure scheme of neglecting third moments about the mean in eq (3). It was shown in part I that this closure scheme does not accurately account for internal uncertain energy transfer and eventually leads to errors in the forecast of the mean. The eddy-damped quasi-normal closure scheme, described in part I and given by the complete set of eq (2)-(4), was used in an additional barotropic predictability experiment. Table 2 shows a comparison of results using the two closure schemes with the same initial conditions. There appears to be no systematic difference in predictability, at least as the term is defined here. However, in a later section we will view predictability from a different angle and we will see a deficiency in the simple closure scheme.

The deterministic vorticity eq (7) neglects the  $\beta$ -effect which is described in relation to the stochastic dynamic

TABLE 2.—Comparison of simple closure (stochastic dynamic) with eddy-damped closure (3-moment) in terms of predictability

Wave number source	Wave number	Stochastic dynamic		3-Moment	
		$\sqrt{\text{var}}=10\%$	$\sqrt{\text{var}}=5\%$	$\sqrt{\text{var}}=10\%$	$\sqrt{\text{var}}=5\%$
(2, 4, 6)	4	(days) 7½	(days) >12	(days) 9	(days) >12
(4, 8, 12)		5	>12	5	9¼
(2, 4, 6)	6	4¼	10¼	4	11
(6, 12, 18)		4½	7½	3¾	5½
(4, 8, 12)	8	3½	5½	3½	5¼
(4, 8, 12)		2¼	4½	2½	4¼
(6, 12, 18)	12	2½	4	2¼	4½

TABLE 3.—Comparison of  $\beta$ -effect in terms of predictability for waves of mode 2

Wave number source	Wave number	No $\beta$ -effect included		$\beta$ -effect included	
		$\sqrt{\text{var}}=10\%$	$\sqrt{\text{var}}=5\%$	$\sqrt{\text{var}}=10\%$	$\sqrt{\text{var}}=5\%$
(2, 4, 6)	4	(days) 8	(days) >12	(days) 7½	(days) >12
(4, 8, 12)		7½	10	5¼	8¼
(2, 4, 6)	6	5½	10¼	5¼	11½
(6, 12, 18)		3½	7½	4½	8
(4, 8, 12)	8	3½	7½	3½	6½
(4, 8, 12)		2¼	5	2¼	4½
(6, 12, 18)	12	1	4¼	2½	3¼

approach in part I. With this included, eq (7) becomes

$$\frac{\partial(\nabla^2\psi)}{\partial t} = -J(\psi, \nabla^2\psi) - \beta \frac{\partial\psi}{\partial x} \quad (10)$$

where  $\beta = df/dy$ ;  $f$  is the Coriolis parameter. The effects of the inclusion of this linear term are shown in table 3 where the simple closure scheme has been used. It is seen that there is little difference in predictability when this is added. (Note that, of the two modes in the  $y$ -direction, mode 2 is shown in table 3.)

### 3. ENERGY SPECTRA AND PREDICTABILITY

Lorenz has used low-resolution spectral models quite successfully to simulate many observed physical features. It is desirable to check the low-resolution model of only three waves against a higher resolution model with regard to predictability. An extension of the stochastic dynamic equations to include more longitudinal wave numbers was performed. The expansion of dependent variables in terms of orthogonal functions was shown in part I where the

TABLE 4.—Barotropic predictability

Wave number	Stochastic dynamic	Lorenz (—%)
	(days)	(days)
2	>7.0	9.2
4	>7.0	4.8
6	5.5	3.7
8	4.6	2.6
10	2.6	2.3
12	1.8	2.0
14	1.6	1.7
16	1.5	1.4
18	1.5	1.3
20	1.0	1.1

functions were given by eq (11). These functions now become

$$\Phi_{00} = 1,$$

$$\Phi_{0m} = \sqrt{2} \cos my/L, \quad m = 1, 2,$$

$$\Phi_{nm} = 2 \cos(nx/L) \sin my/L, \quad m = 1, 2; n = 1, 2, 3, \dots, 15,$$

and

$$\Phi'_{nm} = 2 \sin(nx/L) \sin my/L, \quad m = 1, 2; n = 1, 2, 3, \dots, 15. \quad (11)$$

As pointed out by Lorenz (1963b, 1965), one can consider these waves to "represent" longitudinal wave numbers 2 through 30 on the earth. The stream function  $\psi$  is then expanded in these functions. Because of lack of computer storage, an extension to the baroclinic model was not possible. The extended barotropic model has 62 variables or 62 ordinary differential equations (o.d.e.) in the deterministic form. The stochastic dynamic form of the equations has 2,015 o.d.e. and includes nearly 400,000 nonlinear terms. This is with no third moments.

Table 4 shows results obtained from choosing initial conditions in the same way as for the results shown in table 3. Here, however, the values of  $K_E$  and  $UK_E$  are spread over all 15 waves. Where comparisons are possible, it is seen that there is not a significant difference between using the 3- or 15-wave model, although there is a tendency for slightly longer predictability times using the 15-wave model.

The initial energy distribution in the above example is not realistic (equal energy in all waves), even though the dynamics of the model tend to quickly produce a spectrum with approximately a  $-3$  power law as would be expected from a two-dimensional system (Leith 1968). Thus, it seems that the certain energy transfer between wave numbers, combined with the instability mechanisms, tend to drive any initial spectral state into a preferred state (preferred in some averaged sense by the dynamics of the system). In part I, the major growth of error was emphasized as being due to instability. The nonlinear transfer of energy between a triplet of wave numbers seemed to play a lesser role. To investigate this further, the following

TABLE 5.—*Barotropic predictability*

Wave number	A	B	C	D
	(days)	(days)	(days)	(days)
2	>7.0	>7.0	>7.0	>7.0
4	>7.0	>7.0	>7.0	>7.0
6	5.5	5.2	5.2	5.4
8	4.6	4.0	4.0	4.2
10	2.6	3.3	3.3	3.4
12	1.8	2.8	2.8	2.8
14	1.6	2.4	2.3	2.3
16	1.5	2.0	1.8	1.8
18	1.5	1.7	1.6	1.6
20	1.0	1.6	1.5	1.4

section will consider different initial certain and uncertain energy spectra.

We shall consider that the initial eddy kinetic energy in a wave number,  $K_E(n)$ , can be expressed as a function of the longitudinal wave number  $n$  in the following way:

$$K_E(n) = a \cdot n^{-b}. \tag{12}$$

Wiin-Nielsen (1968) has determined  $a$  and  $b$  by regression calculations using atmospheric data. He found two different regimes for the energy spectra with the partitioning between the two taking place near wave 7. For the wave number range  $1 \leq n \leq 7$ , he found values of  $b$  near  $\frac{1}{2}$ . For the range  $8 \leq n \leq 15$ , he found values of  $b$  near 3. In the following calculations, we assume that there is a set  $(a, b)$  for each range and that, further, wave number 7 is an end point of the regression line for each set. We shall fix the value of  $b$  in the low wave number range and  $b$  for the higher range will be varied for each calculation. An appropriate value of  $a$  can readily be determined to give the total eddy kinetic energy,  $K_E$ , that is desired. According to eq (11), (12), and the above assumptions, that total energy would be given by

$$K_E = a \left( \sum_{n=1}^3 n^{-b_1} + \sum_{n=4}^{15} (3.5)^{b_2-b_1} n^{-b_2} \right) \tag{13}$$

where  $n$  is the integer used in eq (11),

$b_1$  is the low wave number power, and

$b_2$  is the high wave number power.

In our first experiment using eq (13), we use initial values of  $\psi$  such that  $K_Z = 100$ ,  $UK_Z = 1$ ,  $K_E = 100$ ,  $UK_E = 1$ ,  $b_1 = 0.3$ , and  $b_2 = 3$ . This case (hereafter referred to as B) has a  $-3$  power law for the initial certain and uncertain higher wave number energy spectra. Results are shown in table 5 along with the earlier results of the initial "zero" power law shown in table 4 (hereafter referred to as A). Comparing A and B, we see that different initial energy spectra have little bearing on the magnitudes of the predictability values. The largest change in any of the wave number values was 0.6 day. However, one aspect is brought out by these calculations with the  $-3$  power law. Those higher wave numbers in the group  $\geq 6$  tend to become unpredictable, collectively,

at about the same time. That is, wave 20 is 0.6 day more predictable and wave 6 is 0.3 day less predictable.

As another experiment, we use the same initial values as before but change  $b_2$  to equal  $5/3$  in eq (13). This case (referred to as C) has a  $-5/3$  power law for the initial certain and uncertain higher wave number energy spectra. The results shown in table 5 indicate little difference from B. Again, this merely points out that the dynamics of the system, including the barotropic instability mechanism allowed by our choice of zonal flow, drive any initial state into a preferred state.

The following experiment is designed to observe the reorganization of this uncertainty. The same initial values are used as in experiment B; however, the error kinetic energy is distributed according to eq (12) rather than eq (13) with a  $+2$  power law. The results of this case (referred to as D) are shown in table 5 and it is seen that the predictability values are nearly the same as those given by the  $-3$  power law in B. However, the reorganization of each error spectrum changes as the forecast proceeds and these results are shown in figure 1. Initial and resulting spectra after each half-day are indicated, and are the sum of the two  $y$ -modes. Comparing the initial  $-3$  spectrum on the left with the initial  $+2$  on the right, we see that the error growth of the longer waves is slower and that the growth of the shorter waves is faster in the early stages of the  $-3$  case. After 2 days, the two spectra have become very much alike.

The maximum uncertain energy is in the wavelength range predicted to be the most unstable from a linear analysis of barotropic stability (see Wiin-Nielsen 1961). The peak is at  $n=3$  or approximately wave number 6 on the earth—this corresponds to a wavelength of 4666 km at  $45^\circ\text{N}$ . In both cases, the uncertainty in the shorter wavelengths ceases to grow and actually decreases. The results show the effect of the barotropic instability mechanism on the behavior of this simple barotropic fluid and on the uncertainties involved in describing that fluid. The maximum uncertain energy appears in those unstable waves with the greatest amplitude oscillation. The shorter the wave the sooner it becomes unpredictable primarily because of the uncertain advective influence of larger waves and the zonal flow. However, the uncertainty does not grow indefinitely. The dynamics of the fluid only permit the higher wave amplitudes to evolve into a rather restricted structure—the  $-3$  power law in some averaged sense. Thus, the variance is finite and is properly accounted for by the stochastic dynamic equations.

Lorenz (1969) correctly views this end of the error growth as the error becoming as large as the difference between two randomly chosen states; this is essentially the same explanation as above. However, the linear treatment of the error growth by Lorenz (1969) does not account for the nonlinear feedback of uncertain to certain energy that occurs. Those waves which are barotropically stable tend to give up uncertain energy to the zonal flow,

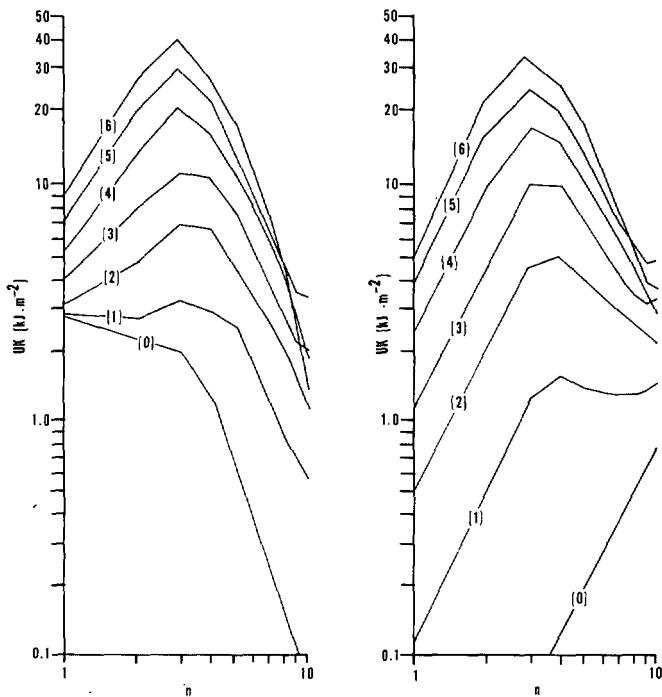


FIGURE 1.—Uncertain energy spectra at half-day intervals with initial  $-3$  power law (left) and initial  $+2$  power law (right).

counteracting and reducing the effect of the advective growth. A stage is eventually reached where the uncertainty is reduced as seen in figure 1. This discussion of certain-uncertain energy transfer and instability is noted in part I.

4. PREDICTABILITY VERSUS RESOLUTION

The present configuration of operational weather forecasting is the so-called "man-machine mix." Of those numerical products used to aid man's final forecast of large-scale sensible weather, still the most used is the numerical forecast of midtropospheric wave patterns. From these patterns (primarily including the 500-mb height forecast), man deduces the general position of weather producing systems and then adds his expertise and/or other numerical products to obtain the details of his forecast. On 500-mb maps, the six or seven large-scale wave patterns around the hemisphere are usually easily identified. However, the shorter scale waves (perhaps most closely characterized by wave number 12) are seen to travel through the longer wave-train and these are the systems that can cause the forecast to be in error—producing sensible weather when none was expected and vice versa, or by significantly displacing the sensible weather several hundred miles. It would seem imperative, then, that the numerical forecast should at least be able to accurately predict the position of wave 12.

We realize that the accurate prediction of sensible weather at a precise point in the space-time domain would involve scales of features with considerably higher wave numbers. Further, for some applications there is utility in knowing only the phase relationships of the lowest order wave numbers. However, in the following we shall

TABLE 6.—Predictability for various rms wind errors (m/s)

Initial error	4.0	2.0	1.0	0.5	0.25
Wave number	(days)	(days)	(days)	(days)	(days)
30	0.0	0.8	1.8	4.0	9.0
28	0.1	0.9	2.0	4.5	9.1
26	0.2	1.0	2.2	5.0	9.2
24	0.3	1.1	2.4	5.3	10.2
22	0.4	1.2	2.6	5.6	11.7
20	0.6	1.3	2.9	5.8	13.0
18	0.8	1.7	3.4	6.0	14.0
16	1.0	2.0	3.7	6.6	14.3
14	1.2	2.4	4.2	7.9	14.6
12	1.4	2.8	5.1	8.8	15.0

confine our interest to the synoptic wave numbers 12 and greater and compare predictability values with decreasing initial error. This is merely of computational convenience to avoid long-term time integrations that would be necessary for wave numbers less than 12.

The initial certain energy values are the same as before; that is, the average kinetic energy per unit mass at 500 mb is taken to be  $200 \text{ m}^2\text{s}^{-2}$  (100 in zonal flow and 100 in the eddy spectrum). The certain energy spectrum will be calculated from eq (13) with a  $-3$  power law and the uncertain spectrum from eq (12) with a zero power law. Previous calculations have specified the initial uncertainty at 500 mb as an average uncertain energy per unit mass of 1 unit each for the zonal and eddy components. This would result in a root-mean-square (rms) vector wind error of 2 m/s or 4 kt. We shall consider now that the initial rms error is 4 m/s and shall successively divide this error by 2 in a series of calculations and inspect the predictability values. In the following calculations, the initial values will satisfy  $UK_z = UK_e$ .

Table 6 shows the predictability values for the various waves. It is seen that halving the error tends to double the predictability times in the smallest wave numbers retained but that the predictability times for the larger wave numbers are not doubled. This effect was found by Lorenz (1969) and was clearly discussed by him. The transfer of error between scales with different doubling times reduces the predictability times in the larger scales. We see, for example, that reducing the original rms error by a factor of 4 increases the predictability of wave number 12 to 5.1 days rather than 5.6.

The results in table 6 for the higher wave numbers are somewhat deceiving (being too optimistic), but have been included to emphasize a point concerning the practical value of predictability. In the atmosphere there is a cascade of energy and enstrophy (see Leith 1968) to the smaller scales. This cascade to higher wave numbers is hindered when the spectrum is arbitrarily cut off for computational reasons. If  $k_*$  is the largest wave number for which amplitudes are computed, then there is a blocking of the energy and enstrophy cascade, and a fictitious build-up occurs on wave numbers less than  $k_*$ .

Of those calculations giving the results shown in table 6, the calculations with extended integrations in time allowed this build-up to reach significant proportions—even though the total energy was conserved to within a

small fraction of 1 percent. The resulting energy in the high wave numbers is too large, which, when coupled to the barotropic instability process, damps the error growth of the smaller, stable scales and extends predictability as defined here. Also, through nonlinear interactions and less relative energy in the unstable waves, this extra energy would tend to extend predictability throughout the spectrum. Thus, the predictability values for the higher wave numbers with progressively smaller initial error are more indicative of a mathematically perfect model than of a two-dimensional fluid.

The problem of the computational cutoff has been dealt with in a number of ways by authors working in numerical modeling. For example, Leith (1971) "simulates" the natural cascade by introducing an artificial viscosity that is dimensionally consistent with the enstrophy cascade rate associated with the  $-3$  power spectrum. The effect of these kinds of procedures on the practical value of predictability has not been considered.

The inclusion of the artificial viscosity, which acts like a minor damping or frictional term, implies that something is being said about the physics of the model. Thus, at every time step, new knowledge is essentially being added. In part I, the effect of this "perfect" parameterization of the physics was discussed, and it was seen to damp the growth of error. The point is that this added artificial viscosity should not damp the error growth, but should increase it because there is "uncertainty" in exactly how that damping term should be incorporated. More important, the damping is only based upon an energy spectrum, the correct spectrum to be sure, but this says nothing about the statistical influence on the *phase* of those wave numbers less than  $k_*$  by the wave numbers greater than  $k_*$ . However, one could add this uncertainty to the cascade simulation by adding another dimension to the  $N$ -dimensional phase space, giving the dimensionless coefficient in the viscosity term a variance (this approach was discussed in part I). This would give more realistic values of predictability versus resolution.

## 5. PREDICTABILITY OF BAROCLINIC SYSTEMS

The earth's atmosphere is not a barotropic system, and any method of deducing the predictability of the atmosphere based upon such a system is only an approximation. This section will consider stochastic predictability experiments using a baroclinic system, but we will first consider previous deterministic studies.

Lorenz (1965) was the first to consider a baroclinic model of the atmosphere. He used the three-wave model that has also been used in this study. Superimposed upon a basic solution, he considered solutions corresponding to small initial random errors. The method of deducing predictability hinged upon a *linear* equation for the growth of errors that gave rise to "error matrices" which could readily be evaluated. The results of the calculations were amplification rates of error for various lengths of time at various periods within a 64-day forecast period.

The important result of this pioneering effort was that the amplification of error was strongly dependent upon

the circulation pattern. There were some 2-day periods where random errors actually diminished and others where it increased by a factor of three. Lorenz points out that there was one 8-day period where errors grew less than threefold, and another where they grew more than fortyfold. Depending upon the definition of a tolerable growth rate, the average predictability could be defined as a week or a month.

A purely numerical study of predictability in terms of the results of several simulation models of the atmosphere was described by Charney (1966). The question posed was how fast will a given error, interpreted as a perturbation of the atmospheric flow, grow before the perturbed motion differs from the unperturbed motion by as much as the difference between two randomly chosen flows? The limit of predictability *in this sense* was found to be greater than 2 weeks. The results of this study have been widely referred to both within and outside of the science of meteorology. The emphasis put on these results is understandable in that there is a considerable amount of physics incorporated into these general circulation models, and they have been able to simulate many observed features of the atmosphere quite well.

There have also been objections raised concerning the above method. Robinson (1967) feels these results give information about the models, but only limited information about the atmosphere. Lorenz (1969) agrees with Robinson that these values are too optimistic in that the effects of the smallest scales (having very short predictability times) are not properly influencing the larger scales. The models use coefficients of turbulent viscosity and conductivity to introduce the statistical effect of unresolved smaller motion on larger scales. Lorenz points out that in such a model the only errors in the small-scale statistics are those resulting from an inadequate knowledge of the large-scale motions that determine them. This criticism is similar to what was said earlier about barotropic predictability with the spectral calculations assumed to be correct. To simulate the difference between atmosphere and model, one must incorporate the limitations of the model and the computational procedure in such a way as to generate uncertainty.

This study has concentrated on the practical values of predictability. It is from this viewpoint that we question the results obtained from the simulation models. We realize that the intent of that study was to consider the long range limit of predictability since it was implicitly assumed that the physical processes of the atmosphere were perfectly known. However, results will be presented suggesting that even if the uncertainties of the small scales were accounted for by the simulation models, the assumption of perfect physics leads to far too optimistic predictability times—at least in the largest scales.

One is tempted to reject those pessimistic predictability values obtained from barotropic calculations because we know the atmosphere has a synoptic climatology. Various areas of the globe have definite weather "patterns" or "histories" which we have been able to explain (in whole or in part depending on the area) as being the result of

various external forces. One must concede that forced dissipative systems are more predictable than those which are not forced. At every time step of the calculation, you are adding new information. However, in a numerical calculation, the last two statements are only true where those physical processes of forcing and dissipation are known and can be "parameterized" in a perfect way. Since we do not know all the physics, nor will we be able to perfectly parameterize these processes for numerical models in the immediate future, it seems necessary to present numerical calculations that will include what these "projected" imperfections in the physics will mean in terms of predictability.

In part I of this study, it was shown how uncertainties of various external parameters could be included in stochastic calculations. Each uncertain parameter could be treated by adding another dimension to phase space, and it was shown how this addition affects the energy equations. Although only a brief qualitative look at the resulting error growth was presented in part I, calculations here show the effects on predictability.

## 6. PREDICTABILITY WITH UNCERTAIN FORCING

The 28-variable two-level model, discussed in part I, is used in the following calculations; it is the same model used by Lorenz (1965) in his baroclinic predictability calculations described above. Lorenz used  $\theta_1^* = 3/32$ ,  $h = 5/32$ ,  $\sigma = 5/128$ , and considered waves 2, 4, and 6. He points out that, if larger wave numbers had been used, there would be a more rapid decay of predictability; on the other hand, the external parameters caused a faster than normal flow that, if reduced, would increase predictability. The values chosen by Lorenz gave the desired nonperiodic flow. Stochastic calculations were performed with many different initial values of the  $\psi$ ,  $\theta$ , and external parameters. The calculations shown here used values of the external parameters  $\theta_1^*$  and  $h$  that were 25 percent less than those used by Lorenz. This was done to achieve a flow more typical of the atmosphere and yet maintain a flow which was nonperiodic. The initial energy values are shown in figure 2. The energy "boxes" contain realistic amounts except for  $A_z$ , which is too large by a factor of about 2. This is discussed below.

If the latitudinal heating parameter,  $\theta_1^*$ , and temperature gradient,  $\theta_1$ , were reduced by a factor of 2, the resulting latitudinal temperature gradient would be in fair agreement with observations. Reduction of the static stability,  $\sigma$ , by a factor of 2 would leave its value in close agreement with that inferred from observations and used by Wiin-Nielsen (1970) in a similar model. Since the value of  $A_z$  is given by

$$A_z = \theta_1^2 / 2\sigma, \quad (14)$$

the effect of reducing  $\theta_1$  and  $\sigma$  by a factor of 2 is seen to reduce the energy by a factor of 2—in agreement with

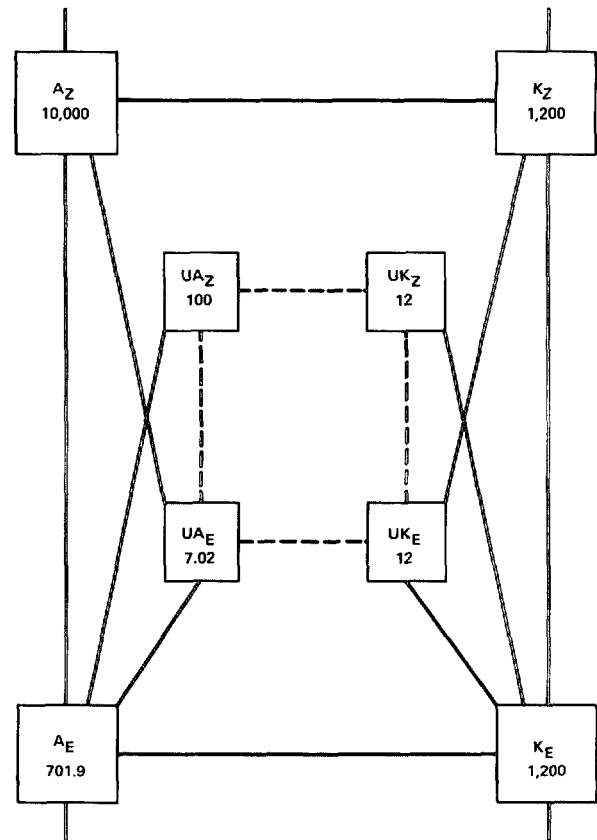


FIGURE 2.—Initial energy values for baroclinic predictability experiments.  $E$  is in  $\text{kJ}\cdot\text{m}^{-2}$ ,  $\dot{E}$  is in  $10^{-4} \text{kJ}\cdot\text{m}^{-2}\cdot\text{s}^{-1}$ .

observations. However, in using such values (along with many different combinations of these and other frictional parameters taken in combination with different sets of wave numbers) we were not able to maintain realistic energy values for the *other* boxes. Wiin-Nielsen (1970) using this same simple model was able to obtain and maintain realistic energy amounts. However, the study by Wiin-Nielsen did not have explicit wave number modes, but rather had an eddy diffusion term to "simulate" the effects of all the longitudinal eddies. We conclude that our failure here is due not to the simple two-level model but to the use of only a limited number of modes.

Our using the larger values of these parameters, as did Lorenz (1965), may not have significantly affected the results. Reduction of such parameters should not greatly affect the time scale of baroclinic instability. An equal decrease in  $A_z$  and the stability tends to have a canceling effect. However, there are indications that this strong forcing and the accompanying strong friction extend predictability times. This is discussed below.

The primary forcing in the atmosphere is that of heating at the Equator and cooling at the poles. This primary forcing, due to radiation processes, is taking place in wave number 0 as defined here. There is also significant heating in this wave number due to the release of latent

TABLE 7.—Baroclinic predictability experiments with primary forcing

Wave number source	Wave number	Adiabatic frictionless	Primary forcing $\sqrt{\text{var}}=10\%$	Primary forcing $\sqrt{\text{var}}=5\%$	Primary forcing $\sqrt{\text{var}}=2.5\%$	Primary forcing $\sqrt{\text{var}}=0.0\%$
		(days)	(days)	(days)	(days)	(days)
(6,12,18)	6	1½	6¾	12¾	15½	17
(2,4,6)	6	4¾	7	12¾	14	20½
(6,12,18)	12	¾	3	4¾	9½	11
(4,8,12)	12	2¾	3¾	4¾	7	10¾

heat in the Tropics. Our simple model has simulated both of these effects by the heating parameter  $\theta_1^*$ . Baroclinic predictability experiments with this parameter uncertain are shown in table 7 where the initial conditions have already been described. It is seen that when the forcing is known perfectly, the stochastic dynamic predictability of wave 6 is over 2 weeks and that of wave 12 is about 10½ days. Again, as pointed out before and in part I, when the generation and dissipation are considered to be computationally perfect, there is a “drainage of uncertainty”—a tendency for the external forces to shrink that ensemble volume in phase space. When this forcing is over-emphasized (as is the case here), the predictability is unrealistically extended. This is quite obvious in table 7 when the adiabatic frictionless case (with no forcing but with the same initial conditions) is compared with the last column having perfect forcing. The adiabatic frictionless case is even less predictable than the barotropic model because we have slightly increased the flow and added baroclinic instability *without* adding new information at each time step by saying something about the external forces.

The above indications suggest that the results in table 7 are too optimistic for those cases with forcing included. That we lose the benefit of precise quantitative values is unfortunate; however, this was due to the severely truncated model and not to the stochastic approach. The most important result indicated in table 7 can still be assessed—the influence of uncertainty in the parameters on the values of predictability. It is seen that there can be significant reductions in predictability times depending upon the magnitude of the uncertainty. The results show a large difference between standard deviations of 10 percent and 5 percent. The current state of the art is probably such that the 10-percent value is appropriate—with the latent heat contribution from the Tropics as the main source of uncertainty. In this case, the predictability is only a week for wave 6. There is a tremendous motivation for continued research on this forcing because, if the standard deviation can be reduced to 5 percent, the predictability increases by another 6 days. This gives further incentive to the deterministic “simulation” studies that are in progress which seem to provide the best research tool for pinpointing these parameters.

TABLE 8.—Baroclinic predictability experiments having secondary forcing and with primary forcing assumed perfectly known

Wave number source	Wave number	Secondary forcing $\sqrt{\text{var}}=20\%$	Secondary forcing $\sqrt{\text{var}}=10\%$	Secondary forcing $\sqrt{\text{var}}=0.0\%$
		(days)	(days)	(days)
(6, 12, 18)	6	12	19½	19½

The effect of latent heat release in the synoptic scales as an additional forcing is crudely simulated here in order to further study predictability when the physics of models becomes more complex and realistic. Table 8 shows results when there is a very small forcing in wave 6. The parameter  $\theta_2^*$  is considered to have the constant value 1/90 but has an uncertainty as indicated. In obtaining these results, we assumed that the primary forcing was known perfectly. One sees that even though the forcing is small, the large value of uncertainty significantly lowers predictability. On the other hand, because the forcing is small, a stage is reached eventually where other sources of error dominate, and further reduction of the uncertainty of that forcing fails to lengthen predictability.

7. PREDICTABILITY IN TERMS OF PHASE ERROR

Our definition of predictability heretofore has been one of convention—related to ratios of uncertain to certain energy. There are perhaps more relevant ways of viewing the value of numerical models in terms of the information they provide. Useful information is the real goal of numerical weather prediction and this can take many forms. The stochastic set of equations provides not just the vector of  $N$ -unknowns (amplitudes of functions or grid point values), but also the complete covariance matrix of these unknowns and all combinations of third moments among the variables. How to usefully interpret this information is a topic in itself. The following will consider one method of using this information and will apply that to the growth of phase error of hydrodynamic waves.

The phase angle of a given wave can be seen directly on an  $x,y$  plane by plotting the amplitude of the cosine term along the  $x$ -axis and the amplitude of the sine term along the  $y$ -axis. The phase angle is then given by  $\arctan(\psi_s/\psi_c)$  where  $\psi_s$  and  $\psi_c$  are the amplitudes of the sine and cosine respectively.

The variances of these amplitudes and their covariance will grow from their initial values, and it is especially informative to use the curves called “ellipses of equal probability” (see Uspensky 1937) to study this growth. These curves are given by the equation

$$\frac{1}{2(1-r^2)} \left( \frac{x^2}{\sigma_1} - 2r \frac{x}{\sqrt{\sigma_1}} \frac{y}{\sqrt{\sigma_2}} + \frac{y^2}{\sigma_2} \right) = l \tag{15}$$

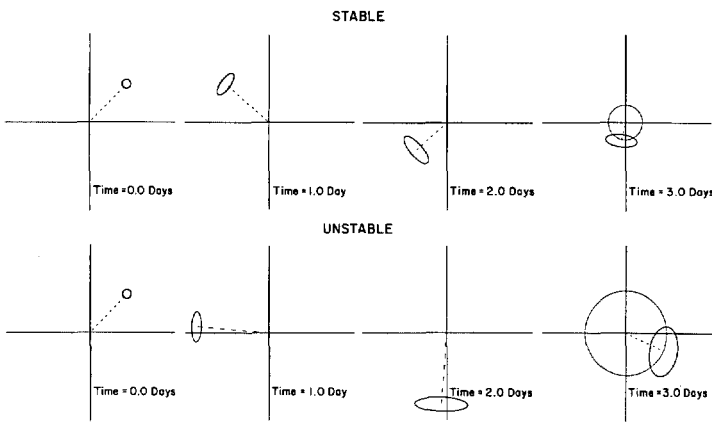


FIGURE 3.—Error growth of wave 6 visualized through ellipses of equal probability in the stable-unstable case.

where  $\sigma_1$ ,  $\sigma_2$ , and  $r$  are respectively variances of  $x$ ,  $y$ , and the correlation coefficient, and where  $l$  is a constant such that  $(1 - e^{-l})$  gives the probability that  $x, y$  are within ellipse  $l$ . Equation (15) implies that the ensemble is multivariate normal. In reality, small third moments are present because of nonlinear energy transfer and this method of display is a slight approximation.

In figure 3 the vector, whose length,  $R$ , is the amplitude of the wave, is drawn from the values of the means of the amplitudes of the sine and cosine of wave 6. The value of  $l$  has been chosen so that the probability is 1/2 that the vector is within the ellipse. It can be shown that the kinetic energy of the wave is proportional to the area of the circle with radius  $R$ . The kinetic energy in wave 6 of this barotropic model is given by

$$K_6 = \frac{1}{2} a_6^2 (\psi_s^2 + \psi_c^2). \tag{16}$$

Amplitude,  $R$ , is given by

$$R = (\psi_s^2 + \psi_c^2)^{1/2}. \tag{17}$$

It follows that

$$K_6 = \frac{a_6^2}{2\pi} \quad (\text{area of circle of radius } R) \tag{18}$$

The changing phase angle indicates the movement of the wave, and it is evident in figure 3 how the uncertainty in the phase of the wave is growing. In noting the orientation of the ellipse, we see that we know the amplitude of the waves better than we know their phase. This was to be expected and is seen in today's deterministic models. This is unfortunate from the user's point of view in that usually he is more concerned with the "timing" of a weather system than its intensity.

The cases shown in figure 3 were discussed in part I. They are three-wave barotropic cases where the initial con-

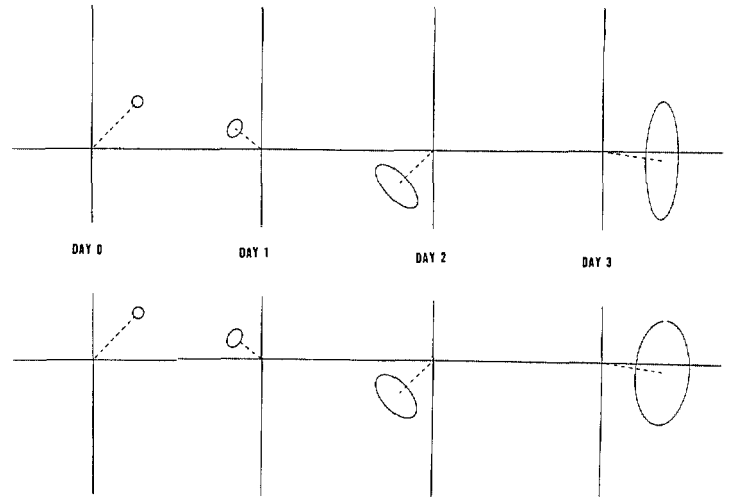


FIGURE 4.—Error growth of a wave from calculations with simple closure (top) and with eddy-damped closure (bottom) for days 0 through 3.

ditions were exactly the same in each except for a sign change in the mode 2 zonal component that changed the barotropic instability criteria. The unstable case had more uncertain energy as discussed in part I, and this is evident in wave 6 of figure 3. However, the relative uncertainty is greater in the stable case. Moreover, if lines are drawn from the origin tangent to the ellipse, the angle between such lines is about  $90^\circ$  for the stable case and about  $70^\circ$  for the unstable case. Thus, if one were concerned about the relative position of wave 6 in this simple model system, the unstable case would be more predictable from this point of view.

A final topic to be considered here is the use of the above method of displaying phase error to look at the effect of the simple closure scheme of Epstein (1969). In part I, it was shown that the closure scheme used by Epstein was congruent in the mean out to about 10 days and that the eddy-damped quasi-normal closure was similarly congruent out to 18 days. In this paper, the predictability values using the two closure schemes (table 2) did not differ too much out to about a week—thus implying congruency in the second-moment terms in that time frame. We shall see below, however, that the second-order congruency breaks down in the simple closure scheme sooner than anticipated.

Figure 4 compares the two closure schemes in a case where the ellipses are shown for days 0 through 3 (results on top are for simple closure and results on the bottom are for eddy damping). Figure 5 is similarly orientated and shows results for days 4 through 7. In figure 4 at day 3, we see that the shapes of the ellipses are beginning to differ. The simple closure scheme gives an ellipse which is more elliptic (greater eccentricity). Figure 5 shows that the eccentricity of the simple closure ellipses has increased. But it is seen that the eddy-damped ellipses do not exhibit this feature and, in fact, at day 7

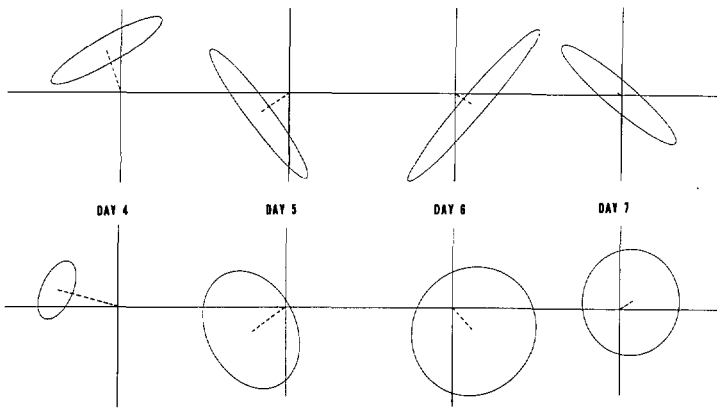


FIGURE 5.—Same as figure 4 for days 4 through 7.

the ellipse is nearly a circle which is perhaps to be expected as the wave vector becomes equally probable in any direction. What happens in the simple closure case is that the correlation coefficient grows unchecked and eventually becomes greater than 1 in absolute value. This, of course, is unrealistic and implies that the covariance matrix is no longer positive-definite. Some eigenvalues associated with the covariance matrix will become very large while others become very small. This in itself is to be expected. If we start with no initial covariances among variables and equal variance for each variable, then we have an  $N$ -dimensional sphere in phase space. Now, as the dynamics of the two-dimensional fluid drive the eddy kinetic energy into the form of a  $-3$  power spectrum in some averaged sense, the uncertain energy spectrum takes on a similar form. Thus, the original sphere loses dimensionality and becomes extremely elongated in a few directions. While this effect might cause ellipses of equal probability to become elongated if wave components of two *different* scales were used, it is not clear why the amplitudes of a sine and cosine of a *single* wave component would become elongated.

The answer to the above failure lies in the results of part I. In dropping third moments in the simple closure scheme, the uncertain energy transfer between uncertain energy forms is not allowed (see part I). This nontransfer occurs because the interaction between uncertain wave numbers obviously involves a third moment (a triplet of waves interact). Also, the interaction between the uncertain eddies and the uncertain zonal flow involves a triple product (barotropic instability). The simple closure scheme has a contradiction, then, of allowing nonlinear interactions between certain components and not among uncertain components. Specifically in this barotropic case, the energy transfer between zonal and eddy components depends entirely on velocity phase relationships—the convergence of the meridional transport of eddy westerly momentum. Thus, the ensemble wave-phase relationship with the zonal flow contains a contradiction when the associated third moment term is dropped. The time evolution of the covariance term relating sine and cosine of a wave is not consistent with the physics of the model.

The use of these ellipses of equal probability in the above way is just a simple example of the many different ways that the predictability and “believability” of numerical forecasts can be viewed.

## 8. SUMMARY AND CONCLUSIONS

There are four points worth emphasizing in concluding this discussion of predictability. The first concerns predictability results based on uncertainties in the initial horizontal wind field; that is, the results using the barotropic vorticity equation. Though the results of the specific linear approach of Lorenz (1969) were highly dependent upon the form of the energy spectrum, the results presented here show that any initial certain or uncertain energy spectra give essentially the same predictability results. This is because the stochastic dynamic equation set is dynamically consistent; that is, they contain the complete dynamics of the two-dimensional fluid, and the fluid dynamics tend to drive any initial state into a  $-3$  power spectrum (in some time-averaged sense).

The second point is that there are indications that improvements in our knowledge of and parameterization of the physical processes of the atmosphere will lead to predictability times considerably longer than those given by barotropic experiments, at least in the planetary scale waves. This is because forced dissipative systems are more predictable than those which are not—at least when the forcing is known considerably well. However, those predictability times of the *medium* and *smaller* scales (e.g., the wave numbers greater than 12) may not improve significantly with improved physics. The uncertainties in the wind field are the primary source of error in these scales. The error growth due to advection, instability, and nonlinear cascade will destroy predictability. The uncertain advecting influence of the zonal flow and of the low wave numbers, and the large errors accompanying instability (baroclinic and barotropic) will be sources of uncertainty from the low wave number side of the spectrum. The cascade down the spectrum of errors in the initial conditions of the smallest resolvable scales plus the additional sources of error generated by the computational wave number cutoff, will introduce errors from the high wave number side. Thus, increased predictability in the medium and smaller scales retained in a mathematical model must mainly come from a more accurate initial specification of the wind field.

The third point is that, for predictability values to be of practical use in justifying observing systems, all sources of error must be taken into account. While forced systems are more predictable, there are uncertainties in the applications of these forces. It was shown in this study and in part I, how the stochastic dynamic equation set can be used to include the external sources of error. In their present form, computations with the stochastic dynamic equation set are too demanding for today’s computers—for other than simple models. Yet, the simple *qualitative* calculations presented here indicate that those uncertainties in the forcing parameters will have considerable

impact on the practical prediction of sensible weather. These effects on predictability have not been considered in a quantitative manner before, but *it is necessary* to consider them if any claims of predictability, or its economic impact, are to be taken seriously. However, for the sake of discussion in the absence of such quantitative data, we shall speculate on the predictability of wave number 12 as it might be 10 yr from now. Though the rms vector wind error has a value of about 4 m/s at 500 mb as a yearly average (verified against selected rawinsonde observations), we will assume that this will be reduced to 2 m/s over the globe. Based upon barotropic results (see table 6) and baroclinic results with an uncertainty in the primary heating of 2.5 percent (see table 7), we would then have a predictability range of about 3–8 days for such an initial error. The 8-day value is rather uncertain, with only the effect of uncertain zonal heating included, as was previously discussed. However, it is not likely that this value would increase too much in the next 10 yr from the inclusion of additional physics in this scale. The complex latent heat and radiation transfer processes occurring on this synoptic scale are a long way from being numerically simulated in a perfect manner. Yet, improvement in this area may ultimately be the most important factor in improving predictability (once the errors in the advection field are proportionately tolerable). Finally, the 3–8 day values were determined from computationally perfect models. The effect of the spatial truncation (on a grid or in spectral form) will be a source of error. The results shown in table 6 for high wave number and small initial error serve as an example of the misleading results that can be obtained from neglect of this source of error. All things considered, we speculate a predictability range of 5–7 days. We stress again that speculation is not a good bargaining tool and that more complicated stochastic dynamic calculations are necessary.

The final point concerns the uses of the stochastic dynamic equations with regard to predictability. The introduction of this paper alludes to the inability of the science of meteorology to establish precise cost-benefit ratios with regard to observing systems. Using the stochastic equations for analysis and prediction and in conjunction with proposed observing systems, it is possible to far more accurately determine such ratios. But the use of the stochastic equations as an operational tool rather than as a research tool seems to be their most important advantage. The globally averaged value of predictability that has been studied by others and included in this study has little meaning to a forecast user. His interest is in how good the environmental information that he has been given is—at the time he wants it and at the place he wants it. Knowledge of the uncertainty of a variable may be as valuable as the variable itself—decisions can be made from that knowledge. As we have seen, the growth of uncertainty depends upon many things and will vary from place to place and from one period to

another. This is what the stochastic dynamic equations provide: based upon the dynamic situation at a given time, the believability of each meteorological variable at any point in space and at any point in time is a predicted quantity.

#### ACKNOWLEDGMENTS

The author is grateful to Edward S. Epstein and C. E. Leith for their helpful suggestions.

Financial support was provided by the United States Air Force and by National Science Foundation Grants GP-4385 and GS-19248. Computations were performed at the National Center for Atmospheric Research (NCAR); the cordial cooperation and support of the entire NCAR staff is gratefully acknowledged. This article was written at the National Meteorological Center, and the author thanks the graphics department of the National Oceanic and Atmospheric Administration and Mary Daigle, who typed the manuscript.

#### REFERENCES

- Charney, Jule G., et al., "The Feasibility of a Global Observation and Analysis Experiment," *Bulletin of the American Meteorological Society*, Vol. 47, No. 3, Mar. 1966, pp. 200–220.
- Epstein, Edward S., "Stochastic Dynamic Prediction," *Tellus*, Vol. 21, No. 6, Stockholm, Sweden, 1969, pp. 739–757.
- Fleming, Rex J., "On Stochastic Dynamic Prediction: I. The Energetics of Uncertainty and the Question of Closure," *Monthly Weather Review*, Vol. 99, No. 11, Nov. 1971, pp. 851–872.
- Julian, Paul R., Washington, Warren M., Hembree, Louis, and Ridley, Cicely, "On the Spectral Distribution of Large-Scale Atmospheric Kinetic Energy," *Journal of the Atmospheric Sciences*, Vol. 27, No. 3, May 1970, pp. 376–387.
- Kao, S.-K., and Wendell, Larry L., "The Kinetic Energy of the Large-Scale Atmospheric Motion in Wavenumber-Frequency Space: I. Northern Hemisphere," *Journal of the Atmospheric Sciences*, Vol. 27, No. 3, May 1970, pp. 359–375.
- Leith, C. E., "Diffusion Approximation for Two-Dimensional Turbulence," *Physics of Fluids*, Vol. 11, No. 3, Mar. 1968, pp. 671–672.
- Leith, C. E., "Atmospheric Predictability and Two-Dimensional Turbulence," *Journal of the Atmospheric Sciences*, Vol. 28, No. 2, Mar. 1971, pp. 145–161.
- Lorenz, Edward N., "Deterministic Nonperiodic Flow," *Journal of the Atmospheric Sciences*, Vol. 20, No. 2, Mar. 1963a, pp. 130–141.
- Lorenz, Edward N., "The Mechanics of Vacillation," *Journal of the Atmospheric Sciences*, Vol. 20, No. 5, Sept. 1963b, pp. 448–464.
- Lorenz, Edward N., "A Study of the Predictability of a 28-Variable Atmospheric Model," *Tellus*, Vol. 17, No. 3, Stockholm, Sweden, Aug. 1965, pp. 321–333.
- Lorenz, Edward N., "The Predictability of a Flow Which Possesses Many Scales of Motion," *Tellus*, Vol. 21, No. 3, Stockholm, Sweden, 1969, pp. 289–307.
- Robinson, G. D., "Some Current Projects for Global Meteorological Observation and Experiment," *Quarterly Journal of the Royal Meteorological Society*, Vol. 93, No. 398, London, England, Oct. 1967, pp. 409–418.
- Uspensky, J. V., *Introduction to Mathematical Probability*, McGraw-Hill Book Co., Inc., New York, N.Y., 1937, 500 pp.
- Wiin-Nielsen, Aksel, "On Short- and Long-Term Variations in Quasi-Barotropic Flow," *Monthly Weather Review*, Vol. 89, No. 11, Nov. 1961, pp. 461–476.
- Wiin-Nielsen, Aksel, "On the Annual Variation and Spectral Distribution of Atmospheric Energy," *Tellus*, Vol. 19, No. 4, Stockholm, Sweden, 1967, pp. 540–559.
- Wiin-Nielsen, Aksel, "A Theoretical Study of the Annual Variation of Atmospheric Energy," *Tellus*, Vol. 22, No. 1, Stockholm, Sweden, 1970, pp. 1–15.